Title	Antibody-based analysis reveals "filamentous vs. non-filamentous" and "cytoplasmic vs. nuclear" crosstalk of cytoskeletal proteins.
Author(s)	Kumeta, Masahiro; Hirai, Yuya; Yoshimura, Shige H; Horigome, Tsuneyoshi; Takeyasu, Kunio
Citation	Experimental cell research (2013), 319(20): 3226-3237
Issue Date	2013-12-10
URL	http://hdl.handle.net/2433/179773
Right	© 2013 Elsevier Inc.
Type	Journal Article
Textversion	author

Research Article

Antibody-based analysis reveals “filamentous vs. non-filamentous” and “cytoplasmic vs. nuclear” crosstalk of cytoskeletal proteins

Masahiro Kumeta[1*], Yuya Hirai[1], Shige H. Yoshimura[1], Tsuneyoshi Horigome[2], and Kunio Takeyasu[1]

[1]Graduate School of Biostudies, Kyoto University, Kyoto 606-8501, Japan
[2]Graduate School of Science and Technology, Niigata University, Niigata 950-2181, Japan

Abstract
To uncover the molecular composition and dynamics of the functional scaffold for the nucleus, three fractions of biochemically-stable nuclear protein complexes were extracted and used as immunogens to produce a variety of monoclonal antibodies. Many helix-based cytoskeletal proteins were identified as antigens, suggesting their dynamic contribution to nuclear architecture and function. Interestingly, sets of antibodies distinguished distinct subcellular localization of a single isoform of certain cytoskeletal proteins; distinct molecular forms of keratin and actinin were found in the nucleus. Their nuclear shuttling properties were verified by the apparent nuclear accumulations under inhibition of CRM1-dependent nuclear export. Nuclear keratins do not take an obvious filamentous structure, as was revealed by non-filamentous cytoplasmic keratin-specific monoclonal antibody. These results suggest the distinct roles of the helix-based cytoskeletal proteins in the nucleus.

Highlights
* A set of monoclonal antibodies were raised against nuclear scaffold proteins
* Helix-based cytoskeletal proteins were involved in nuclear scaffold
* Many cytoskeletal components shuttle into the nucleus in a CRM1-dependent manner
* Sets of antibodies distinguished distinct subcellular localization of a single isoform
* Nuclear keratin is soluble and does not form an obvious filamentous structure

Keywords
cytoskeleton, keratin, monoclonal antibody, nuclear matrix, nuclear scaffold, nuclear transport

Abbreviations
LMB, leptomycin B; NES, nuclear export signal; NLS, nuclear localization signal; NPC, nuclear pore complex

*Corresponding author: Masahiro Kumeta
Phone/Fax: +81-75-753-7905
E-mail: kumeta@lif.kyoto-u.ac.jp

Introduction

The existence of functional scaffold in the nucleus has been long debated based on the results of several different methodologies. Observation of chromatin-depleted cell nucleus by electron microscope revealed a network of branched 10-nm fibers distributed throughout the nucleoplasmic space [1]. Biochemical fractionation techniques have been developed to uncover the structural basis of the nuclear organization by sequential elution of soluble proteins [2]. As an outcome of this step-by-step dissection, 80-nm beaded fibers were observed in high-salt extracted nucleus, and 10- to 20-nm thin fibers along with 500- to 750-nm large lobes were observed in chromatin-depleted nucleus by atomic force microscopy [3]. Recent proteomic studies have identified the protein composition of nuclear structures resistant to biochemical treatments [4-6]. More than 400 proteins were identified, including many novel and uncharacterized proteins such as BXDC1 (brix-domain containing 1), EBNA1BP2 (EBNA 1 binding protein 2), and Caprice (C19orf21). This implies that previously limited understanding of biochemically stable protein complexes obtained by normal molecular biology approach is due to their highly insoluble properties.

Various cytoskeletal proteins have been found to shuttle between the cytoplasm and the nucleus and to play a role in nuclear-specific events such as transcription, DNA repair and nuclear body formation [7]. Two typical examples of such proteins are nuclear actin and β-catenin, which are indispensable for RNA polymerases and chromatin remodeling [8] and for transmitting Wnt signal into the nucleus [9], respectively. Another example identified in our group is cell cycle-dependent nuclear accumulation of an actin-binding cytoskeletal protein actinin-4 and its interaction with the INO80 chromatin-remodeling complex [10]. Such findings imply that nucleus and cytoplasm are closely linked by the nuclear shuttling of scaffold components. Interestingly, in spite of those shuttling proteins' crucial role in the nucleus, they often do not exhibit apparent nuclear localization and are dominantly localized to the cytoplasm.

In this study, we have raised a variety of monoclonal antibodies against crude nuclear scaffolding proteins prepared by biochemical fractionation of the cells. Molecular analyses using these monoclonal antibodies indicate a close relationship between cytoskeletal proteins and nuclear scaffold, including a CRM1-dependent nuclear localization of non-filamentous keratins, and provide novel insights into the dynamic structural scaffold of the nucleus.

Materials and Methods

Preparation of immunogen, immunization, and cloning of hybridoma

Mitotic chromosomal proteins were a gift from Dr. K. Fukui, which were isolated as previously described [11]. High-salt extraction fraction and highly insoluble fractions were prepared based on the method described previously [2], by the sequential treatments of HeLa S3 cells with buffer A (10 mM PIPES-NaOH (pH 6.8), 100 mM NaCl, 300 mM sucrose, 3 mM $MgCl_2$, 1 mM EGTA, 0.5% Triton X-100, 1 mM PMSF, and 1:100 protease inhibitor cocktail (Nacalai Tesque)), buffer B (10 mM PIPES-NaOH (pH 6.8), 250 mM $(NH_4)_2SO_4$, 300 mM sucrose, 3 mM $MgCl_2$, 1 mM EGTA, 0.5% Triton X-100, 1 mM PMSF, and 1:100 protease inhibitor cocktail (Nacalai Tesque)), and buffer C (10U/μl deoxyribonuclease I (DNase I) in 10 mM PIPES-NaOH (pH 6.8), 50 mM NaCl, 300 mM sucrose, 3 mM $MgCl_2$, 1 mM EGTA, 0.5% Triton X-100, 1mM PMSF, and 1:100 protease inhibitor cocktail (Nacalai Tesque)).

The immunization and cell fusion processes were performed at Immuno-Biological Laboratories (IBL) and Takara Bio. BALB/c mice were immunized by intradermal and subcutaneous injections. After 4 and 8 weeks, the immunoreactivities of the antisera were examined by enzyme-linked immunosorbent assay (ELISA), immunoblot and immunofluorescence microscopy. A mouse with the highest titer was chosen for making hybridoma cells. The spleen cells were harvested and fused with myeloma cells (X-63Ag8) by PEG-mediated method. The fused hybridoma cells were cultured in TIL medium (IBL) supplemented with 10% fetal bovine serum in 5% CO_2 at 37°C. The cells were cloned by limited dilution and the culture media were subjected to screening by immunostaining of HeLa cells. Positive clones were selected and further cultured.

Immunostaining and microscopic observation

HeLa cells were treated with buffer A for 15 minutes or 20 ng/ml leptomycin B (Calbiochem) for 4 hours. The cells were washed twice with PBS and then fixed with 4% paraformaldehyde (PFA) in PBS at room temperature for 15 minutes. The sample was blocked with 5% normal goat serum for 15 minutes, and then incubated with the primary antibody. For both non-treated and LMB-treated cells, 0.5% Triton X-100 was added to the blocking buffer for permeabilization. The specific binding was detected by FITC-conjugated anti-mouse IgG (Cappel) or anti-rabbit IgG (Cappel). If necessary, the sample was stained with hoechst 33342 or propidium iodide (PI) (5 μg/ml) in the

mounting medium (Vectashield). Microscopic observations and fluorescent recovery assays were performed at room temperature using a confocal laser scanning microscopes (LSM 5 PASCAL, Carl Zeiss, and FV-1200, Olympus) with ×63 Plan-Apo objective lens N.A. =1.4.

cDNA constructs and recombinant proteins

Complementary DNA for actinin-4, βI-spectrin, keratin-7, -8, -17, -18, and vimentin were amplified from HeLa cDNA pool reverse transcribed by SuperScript II reverse transcriptase (Invitrogen) from total RNA extracted by RNeasy RNA extraction kit (Qiagen). The cDNAs were cloned into pEGFP-C1 vector (Clontech) and transformed into HeLa cells by Effectene transfection reagent (Qiagen) according to the manufacturer's instructions. For bacterial expression, the cDNAs were cloned into pGEX-6P vector (GE) and expressed in BL21RIL *E. coli*.

cDNA expression library screening

The expression library screening was performed by using Lambda-ZAP HeLa cDNA expression library (Stratagene-Agilent) according to the manufacturer's instructions. After transferring the expression library onto the PVDF membrane, conditioned media from hybridoma cells were used for immunoblotting followed by alkaline phosphatase-conjugated anti-mouse IgG (Nacalai Tesque) and detection by nitro blue tetrazolium/3-bromo-4-chloro-5-indolyl phosphate reagent. The phage isolation step was repeated several times to obtain a single clone. The isolated cDNA was identified by an automated DNA sequencer (Beckman) and NCBI BLAST search.

Immunoprecipitation

HeLa cells were resuspended in RIPA buffer (50 mM Tris-HCl (pH 8.0), 150 mM NaCl, 1 mM EDTA, 0.1% SDS, 0.1% deoxycholate, 1% Triton X-100 and 1:100 protease inhibitor cocktail (Nacalai Tesque)) and sonicated. After centrifugation at 15,000 rpm (20,400×g) for 10 minutes, the supernatant was collected. The antibody for the assay was incubated with Dynabeads Protein A (Veritas) at 4°C for 6 hours. Antibody-coated beads were incubated with the supernatant at 4°C overnight. The collected beads were washed five times with the RIPA buffer, and applied to SDS-PAGE followed by Coomassie Brilliant Blue (CBB) staining or Western blotting analysis.

HPLC

Nuclear matrix fraction (8.8 mg) and S2 fraction (12 mg) extracted from HeLa cells were solubilized with 5% SDS supplemented with 2-mercaptoethanol (1: 20, v/v), and heated at 100°C for 5 minutes. After cooling, the solution was supplemented with final 90% (v/v) formic acid, diluted with an equal volume of solvent A (60% formic acid), and centrifuged at 6,500×g for 10 minutes. The supernatant was applied to a 10 μm polystyrene Poros 10 R1 column (7.5 mm × 75 mm; PerSeptive Biosystem, Cambridge) equilibrated with solvent A. The proteins were then eluted with a 0 to 35% linear gradient of solvent B (33% n-butanol in 60% formic acid) for 140 minutes. The concentration of solvent B was increased to 45% in 10 minutes, then increased to 100% in 5 minutes, and was kept at 100% for 20 minutes. All the steps were performed at 1.5 ml/minute flow-rate at room temperature. The aliquots of the sample were concentrated with a centrifugal concentrator. Before the sample was completely dry, 200 μl of water was added, and the drying was continued. This step was repeated three times. The pellets were solubilized with 10% SDS containing 20 mM Tris-HCl (pH 9.0) and 10 mM dithiothreitol, and applied to SDS-PAGE.

In gel digestion

The SDS-PAGE gels were stained with CBB and the excised target bands were cut into small pieces. The gel pieces were destained with 50% acetonitrile in 50 mM ammonium bicarbonate for 10 minutes at 37°C, and sequentially incubated in 100% acetonitrile and water, until CBB faded out completely (3-5 cycles). The gel pieces were then dried in a centrifugal concentrator and rehydrated by 8 μg/ml trypsin (Promega) in 17 mM ammonium bicarbonate. After the trypsin solution was completely absorbed into the gel pieces, minimum amount of 50 mM ammonium bicarbonate was added and incubated for 16 hours at 37°C. The tryptic peptides were extracted twice with 50 μl of acetonitrile/water/trifluoroacetic acid solution (66:33:0.1, v/v) in a sonicator for 10 minutes. The gel pieces were finally dehydrated for 10 minutes with 50 μl of acetonitrile, which was also collected and combined with the extract. The combined extracts were dried at 50°C in a centrifugal concentrator.

Protein identification by matrix-assisted laser desorption ionization-time of flight mass spectrometry (MALDI-TOF MS)

Mass spectra data of tryptic peptides were obtained by using a MALDI-TOF MS (AXIMA-CFR; Shimadzu Biotech, Kyoto) in the positive ion reflectron mode. α-Cyano-4-hydroxycinnamic acid was used as a matrix. The corrected mass lists were used as peptide mass fingerprinting data for search in databases. Mascot search engine (Matrix Science) was used to identify the protein by searching in entries under the Homo

sapience category of the SwissProt databases using the assumptions that peptides are monoisotopic and carbamidomethylated at cysteine residues. Up to one missed trypsin cleavage was allowed. Mass tolerance of 0.5 Da for monoisotopic data was set as the window of error allowed for matching the peptide mass values. Proteins matched with probability value less than 0.05 by probability-based MOWSE score provided from MASCOT were considered to be identified with high reliability.

Protein identification by liquid chromatgography-MS/MS (LC-MS/MS)

The tryptic peptides were analyzed with a nanoflow LC-iontrap-tandem mass spectrometer (nLC-IT-MS/MS, Agilent 1100 LC/MSD Trap XCT Ultra) equipped with an enrichment column (0.3 x 5 mm, ZORBAX 300 SB-C18, 5 μm), an analytical column (0.075 x 150 mm, ZORBAX 300 SB-C18, 3.5 μm), and a spray needle. The peptides were eluted with solvent C (0.1% formic acid) and solvent D (acetonitrile containing 0.1% formic acid), by a 30 minutes linear gradient from 2% to 50% solvent D, followed by 50% solvent D isocratic run for 10 minutes and subsequent 80% solvent D isocratic run for 10 minutes, at a flow rate of 300 nl/minute. The mass spectrometer was operated in positive ion mode over the range of 350-1800 m/z in the data-dependent mode to select the three most intense precursor ions for acquisition of MS/MS spectra. The identification of proteins was performed with Spectrum Mill MS Proteomics Workbench platform (version A.03.02; Agilent Technologies). The data analysis was performed with the following parameters: fixed modification, carbamidomethylation; MH+ range, 600-4000 Da; sequence tag length, more than 1; window setting of merging spectra from the same precursor, retention time within ±15 s and mass value within ±1.4 m/z; maximum charge, +7; minimum S/N, 25. The extracted and processed MS spectra were searched against the in-house built IPI human protein database. Carbamidomethylation was set as fixed modification, and oxidized methionine as variable modification. Mass tolerance was ±2.5 Da on MS peaks and ±0.7 Da on MS/MS peaks. Two missed cleavages with trypsin were allowed. The instrument setting was specified as electrospray ionization (ESI) ion trap. Proteins with more than two plausible peptides matches (the peptide score more than 6 and SPI more than 70%) were considered to be identified.

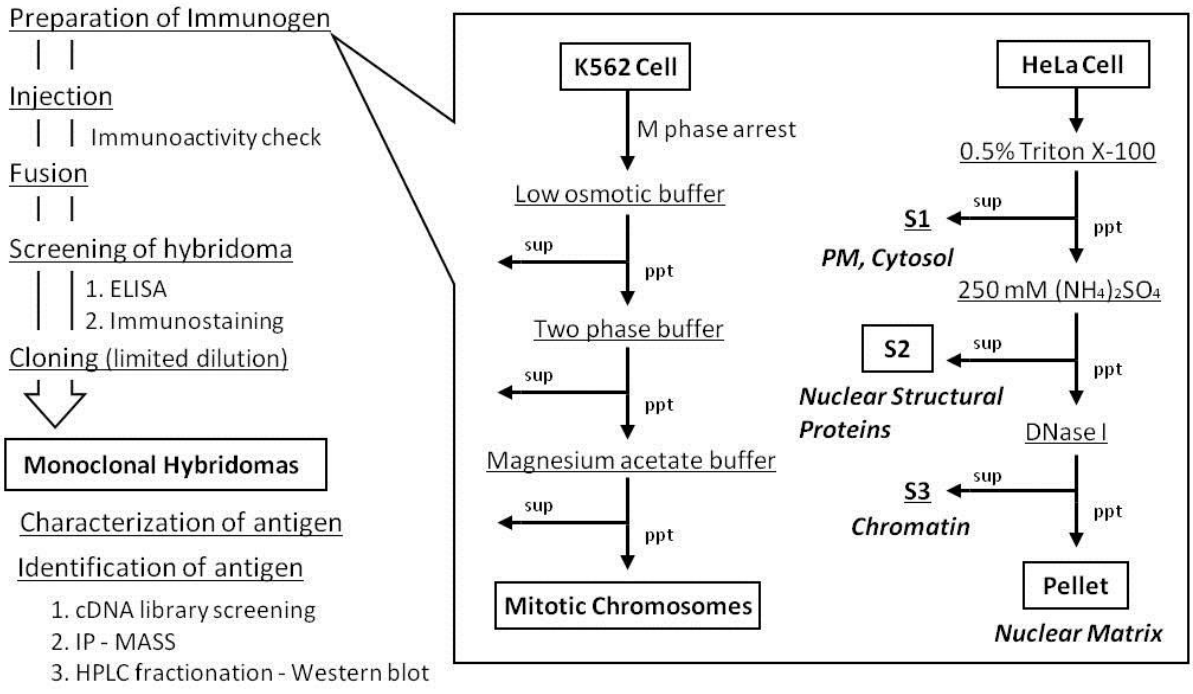

Fig. 1 Overview of the experiments and preparation of immunogen.
Three fractions of biochemically-stable nuclear structural protein complexes, *i.e.*, Mitotic Chromosomes, S2 and Pellet, were extracted and used as immunogens. Hybridoma cells were screened by immunofluorescence and cloned by limiting dilution. Antigens for each monoclonal antibody were identified by cDNA expression library screening, immunoprecipitation followed by mass spectroscopy, or immunoblotting against known protein samples.

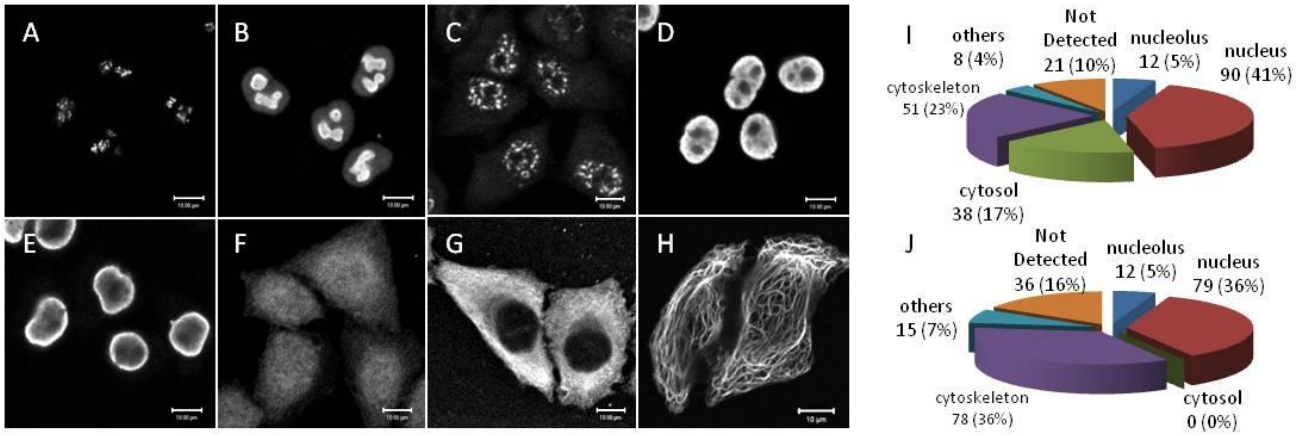

Fig. 2 Immunostaining of HeLa cells by a set of monoclonal antibodies.
(A-H) HeLa cells grown on a cover glass were fixed with 4% PFA and subjected to immunostaining with the culture media of monoclonal hybridomas. The immunosignals were found in a variety of subcellular compartments: nucleus, nucleolus, nuclear membrane, nuclear speckles, and cytoplasmic substructures. Scale bars: 10 µm. Antibody ID: (A) 2-30C, (B) 3-81A2, (C) 45A, (D) 1-67D, (E) 58A, (F) 90A, (G) 54I, (H) 2-40D. (I) Summary of the immunostaining results of HeLa cells fixed with 4% PFA. (J) Summary of the immunostaining of HeLa cells treated with buffer containing 0.5% Triton X-100 before fixation.

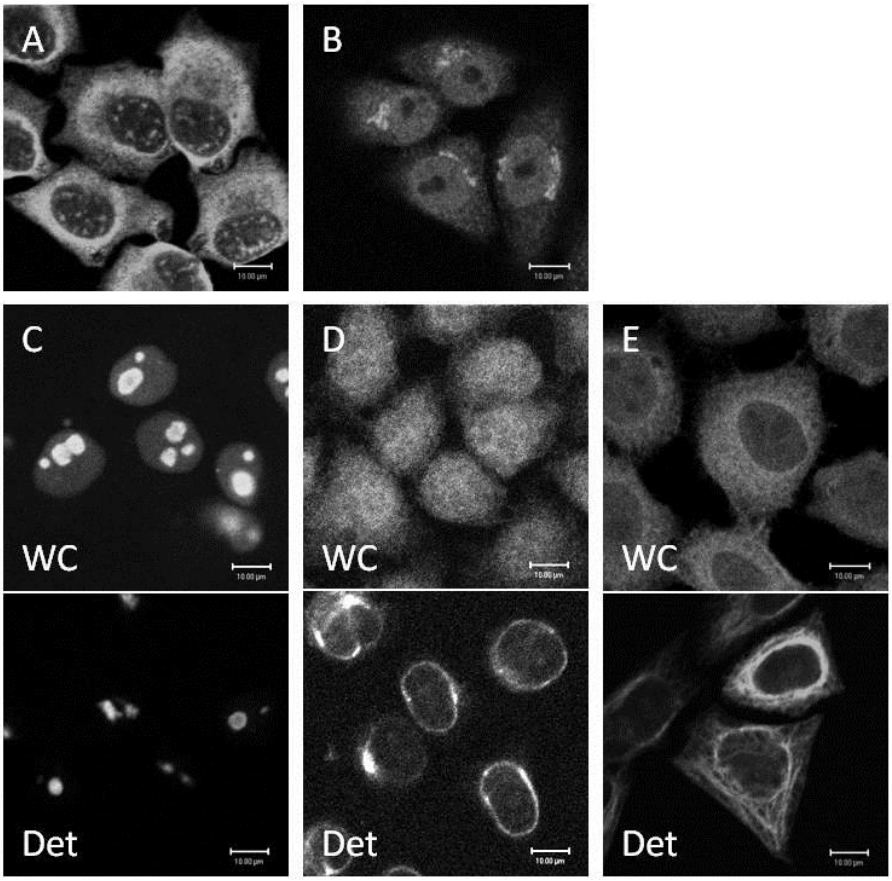

Fig. 3 Characteristic localizations of antigens revealed by immunostaining of HeLa cells.
(A,B) Antigens localized to more than two subcellular compartments: nuclear speckle and cytoplasm (A; 31C), nucleoplasm, cytoplasm and subnuclear compartment (B; 2-63A). (C-E) Antigens which showed more than two biochemically-distinctive molecular populations by buffer A treatment. Antibody ID: (C) 15D-D, (D) 36C, (E) 1-93A. WC: immunofluorescence staining of whole cells fixed with PFA, Det: cells treated with buffer A before the fixation. Scale bars: 10 µm.

Results

Monoclonal antibody-based approach to the analysis of biochemically-stable nuclear scaffold

Using the three fractions of nuclear structural proteins extracted from cultured cells as immunogens (Fig. 1), we aimed to obtain several different monoclonal antibodies against nuclear scaffold proteins, with the goal of producing specific antibodies that recognize distinct states of the antigen. After a limiting dilution of the obtained hybridomas, the first screening was performed by ELISA, and culture media were collected for immunofluorescence microscopy. Some of the beautiful and intriguing staining patterns are shown in Fig. 2. Half of the antibodies recognized nuclear structures and the rest recognized cytoplasmic structures (Fig. 2I). Some of the antibodies showed immunosignals in more than two distinctive subcellular compartments (Fig. 3A,B). Among the nuclear antibodies, a quarter of them were also found to recognize cytoplasmic structures, which indicated the role of such structural proteins in both the cytoplasm and the nucleus. When the cells were pre-treated with the buffer containing 0.5% Triton X-100 to remove highly soluble proteins, some of the antibodies showed altered localization of immunosignals (examples in Fig. 3C-E and summarized in Fig. 2J). These results suggest that biochemically distinctive multiple populations of the antigens exist in cells, and that it is possible to identify individual localizations of the scaffold proteins by separating these populations.

Molecular composition of the functional scaffold for the nucleus

Antigens for the obtained antibodies were identified by the following methods: 1) cDNA expression library screening; 2) immunoprecipitation followed by the mass spectrometry analysis (Fig. 4); and 3) comparative analysis of immunoblotting band pattern with previously identified HeLa nuclear matrix proteins or highly insoluble rat liver proteins fractionated by reverse-phase HPLC (Fig. 5) [5, 6] (Table 1). The direct reactivity of each antibody against antigen was verified by Western blot using recombinant antigenic proteins. Many of them were already known to serve as functional scaffolds, such as scaffold attachment factor A (SAF-A), which functions as chromatin scaffold by binding to a scaffold attachment region of genomic DNA [12], and nuclear mitotic apparatus protein (NuMA), which is an essential protein for both interphase and mitotic chromatin organization [13]. A number of cytoskeletal components were identified, especially that of intermediate filaments including lamins, keratins, and vimentin. The large number of identified intermediate filament components is reasonable, because intermediate filaments are known to be the most biochemically stable structures among cytoskeletons. Interestingly, multiple numbers of monoclonal antibodies were found to recognize the same protein,

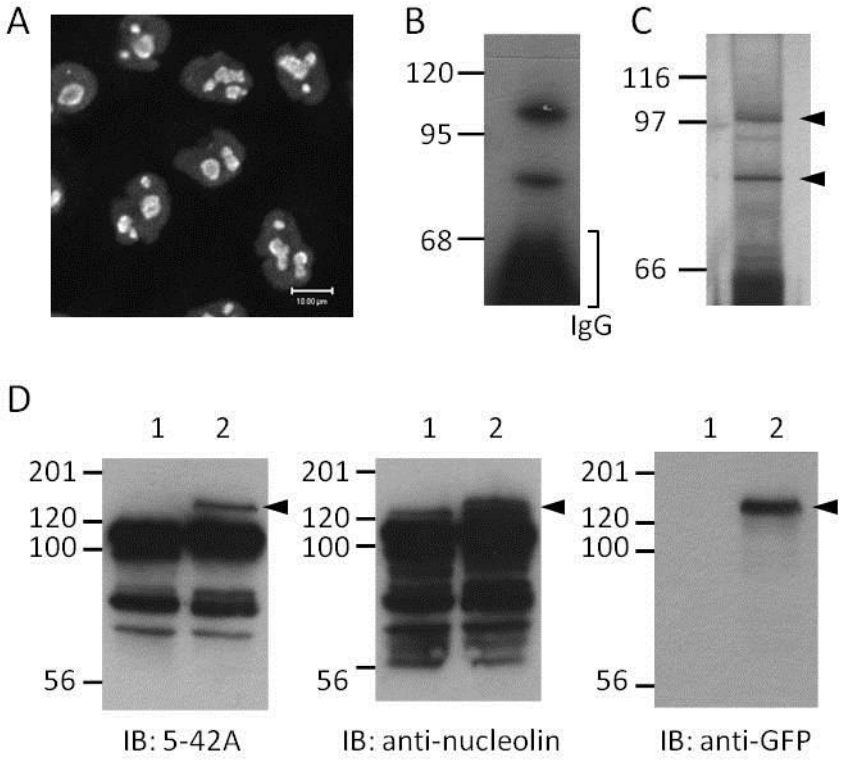

Fig. 4 Identification of 5-42A antigen by immuno-precipitation and verification by Western blot.
(A) Immunostaining of HeLa cells with 5-42A antibody. Scale bar: 10 μm. (B) Western blot of 5-42A immunoprecipitated proteins by 5-42A antibody. A band below 68kDa was IgG heavy chain. (C) Silver staining of 5-42A immunoprecipitated proteins. Two bands indicated by arrowheads were subjected to in-gel digestion and mass spectrometry, and identified as nucleolin. (D) Western blot analyses with 5-42A, anti-nucleolin, and anti-GFP antibodies against lysates of HeLa cells (lane 1) and HeLa cells expressing GFP-nucleolin (lane 2). Bands correspond to GFP-nucleolin are indicated by arrowheads.

and many antibodies recognized keratins, nucleolin, and SAF-A, suggesting that these proteins have highly antigenic properties.

The most important outcome of our monoclonal antibody production effort is that several characteristic antibodies recognize the same antigens, but stain different parts/compartments within the cells. One such case is antibodies against actinins and keratins, which exhibited intriguing subcellular distributions. Antibodies 28C and 92B, both of which recognized actinin-4, exhibited cytoplasmic and nucleoplasmic signals, respectively, whereas the major population of actinin-4 detected by a polyclonal antibody largely co-localized with β-actin at the cell adhesion sites (Fig. 6). This is in a strong contrast to the case of nucleolin; the immunolocalizations by many anti-nucleolin antibodies were almost the same. The epitopes of the monoclonal antibodies 28C and 92B were shown to overlap with vinculin-binding site of actinin-4, suggesting that only a vinculin-free population of actinin-4 molecules is recognized by these antibodies [10]. The antibodies against keratins also showed distinct, either cytoplasmic or filamentous, immunolocalizations (Table 1). The antibodies obtained in this study will provide important clues in the future research of subcellular dynamics of scaffold proteins.

CRM1-dependent nuclear shuttling of cytoskeletal proteins

Complementary DNAs encoding actinin-4, βI-spectrin, keratin-7, -8, -17, -18, and vimentin were cloned into the GFP-fusion expression vector and introduced into

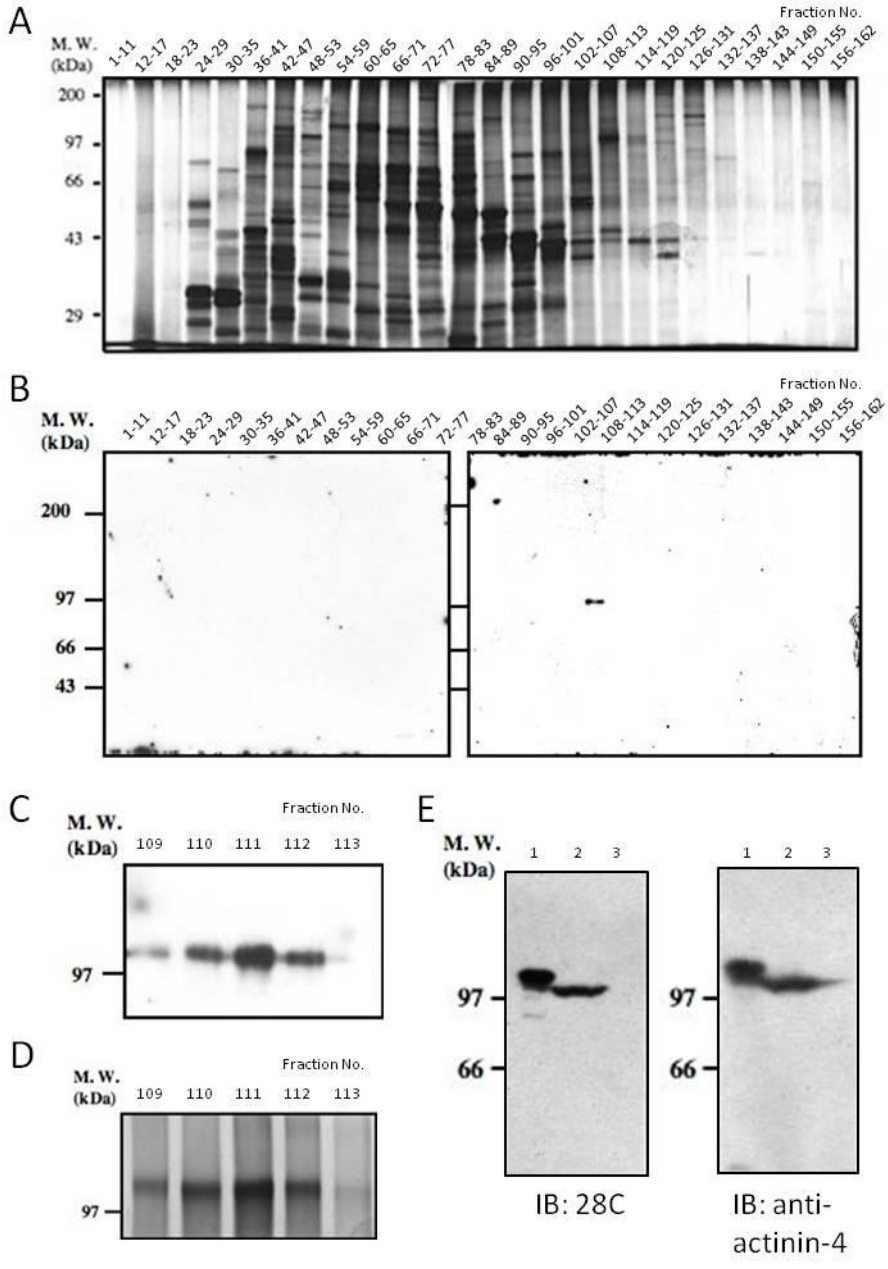

Fig. 5 Identification of 28C antigen by western blot against fractionated nuclear matrix proteins.
(A) Nuclear matrix fraction was separated by reverse-phase HPLC in 60% formic acid and SDS-PAGE. Five to ten fractions were combined and loaded. (B) Western blot analysis of 28C antibody against fractionated nuclear matrix proteins. A band was detected in a lane 108-113. (C) The fractions 109 to 113 was separately loaded and subjected to the Western blot by 28C. (D) Silver staining image of the fractions 109 to 113. The band had been identified as actinin-4 in our previous study [4]. (E) Verification by Western blot. His-tagged recombinant actinin-4 (lane 1), HeLa nuclear matrix proteins (lane 2), and BSA (lane 3) was loaded on SDS-PAGE and immunoblotted by 28C and anti-actinin-4 antibodies.

HeLa cells. All of them showed cytoplasmic filamentous distributions and did not show apparent nuclear localizations (Fig. 7A). Leptomycin B (LMB) is an inhibitor for CRM1, a nuclear export-mediator that exports a wide range of proteins containing a nuclear export signal (NES) [14]. When the HeLa cells were treated with LMB, some of these GFP-fusion proteins exhibited nuclear signals (Fig. 7B). More than 50% of the cells exhibited strong nuclear accumulations of GFP-fused actinin-4 and keratin-8. Moreover, slightly increased nuclear signals were found for keratin-7, -17 and -18, whereas βI-spectrin and vimentin did not exhibit detectable nuclear signals at these experimental conditions. These nuclear accumulations did not result from the digestion or degradation of the GFP-fused proteins, as the apparent size of the GFP-fused proteins did not change after the LMB treatment as shown by the Western blot (Fig. 7C). Keratin-8 and -18 contain the following NES-like sequences: LMNVKLALDI (keratin-8, 377-386 amino acid residues) and LRRTVQSLEI (keratin-18, 299-308). When the GFP-fused keratin-8 and -18 lacking the NES-containing portion were expressed in HeLa cells, they showed obvious nuclear signals (Fig. 7D). This suggests the nuclear targeting property of the N-terminus part of keratins. Actinin-4 exhibited the same property [10]. Fluorescent recovery after photobleaching (FRAP) analysis revealed their nuclear shuttling properties after bleaching the entire nuclear signals (Fig. 7E). They exhibited significant fluorescent recovery during the observation time, demonstrating their continuous exchange through the nuclear pore (Fig. 7F). To summarize, several cytoskeletal scaffold components are actively shuttling in and out of the nucleus, and are exported by the CRM1-dependent pathway.

Nuclear keratins: filamentous vs. non-filamentous forms and cytoplasmic vs. nuclear localization

Table 1 - A list of antigens.

Antigen	Antibody ID#	Localization (immunostaining)	Helix-based motif	Proteomics	
				nuclear matrix [4][5]	mitotic chromosomes [11]
TCOF1 (treacle)	2-30C	nucleolus (FC)		O	
Nucleolin	3-81A2, 5-35C, 5-42A, 5D-F2, 15D-A, 15D-D, 15D-E, 15E-A, 127B*, 127C*	nucleolus (GC)		O	O
SAF-A (SP120)	1-67B, 1-67D, 4-39E1, 4-39E2	NP		O	
Lamin A/C	2-63A, 2-63B, 162B*	NP+CP	coiled-coil	O	O
SFPQ	4D-B	NP		O	
Rad 50	33A	NP	coiled-coil		O
Nuclear mitotic apparatus protein (NuMA)	45A	nuclear speckles	coiled-coil	O	O
RUFY 1	162B*	NP+CP			
ATP binding RNA helicase	150C	CP		O	
α-Actinin 1	28C*	CP	spectrin-repeat		
α-Actinin 4	17C-A, 92B	NP	spectrin-repeat	O	O
	28C*	CP			
βI-Spectrin	4A*	NP+CP dot	spectrin-repeat	O	
Plectin	16G-D1	NP	spectrin-repeat		
	4A*	NP+CP dot			
Bullous pemphigoid antigen 1 eB (BPAG1e)	4A*	NP+CP dot	spectrin-repeat		
Ribosomal protein SA	4A*	NP+CP dot		O	
	39C, 69A	CP			
Keratin 7	107A, 1-93A*, 1-93C*	CP	coiled-coil	O	
	1-33A*, 1-33B*, 4-36A*, 4-36C*, 4-36D*, 7D-A*, 7D-B*, 7D-C*, 21D-A2*	CSK			
Keratin 8	1-21A, 1-93A*, 1-93C*	CP	coiled-coil	O	O
	1-33A*, 1-33B*, 2-40D, 3-47A, 3-47C1, 3-47C2, 3-95A, 3-95B, 3-95C, 4-36A*, 4-36C*, 4-36D*, 4-63A, 7D-A*, 7D-B*, 7D-C*, 21D-A2*	CSK			
Keratin 17	5-42B*	CP	coiled-coil	O	O
Keratin 18	4-4A, 4-4B, 4-4D, 4-4E, 5-35B, 5-35E, 5-42B*	CP	coiled-coil	O	O
	5-22C	CSK			
Vimentin	54I	CP	coiled-coil	O	O

*: antibody with more than two antigens, O: proteins identified by the proteomics analysis

NP: nucleoplasm, CP: cytoplasm, CSK: cytoskeleton, FC: fibrillar center, GC: granulcar component.

There are 20 subtypes of keratin genes in humans and their expression is regulated in a cell type-specific manner [15]. Keratin-7, -8, -17, and -18 are known to be expressed in HeLa cells. Both antibodies 1-21A and 2-40D specifically recognized keratin-8 on Western blot, but exhibited different immunolocalizations by cell staining; 2-40D recognized a structure that was obviously filamentous, whereas 1-21A exhibited cytoplasmic localization (Fig. 8A,B). When the cells were pre-treated with LMB, only the antibodies that recognized non-filamentous cytosolic keratins showed nuclear signals (Fig. 8C). The antibodies specific to filamentous keratins did not exhibit nuclear signals after the LMB treatment, suggesting that nuclear keratins do not take the filamentous form identical to their cytoskeletal state. When the soluble fraction of proteins was removed from the cells by the buffer containing 0.5% Triton X-100 after LMB treatment, the nuclear signals were not detected. 1-21A antibody exhibited filamentous signals in the 0.5% Triton X-100-treated cells, indicating that this antibody recognizes both filamentous and non-filamentous forms of keratin-8. These findings reveal the CRM1-dependent nuclear shuttling of soluble and non-filamentous keratins.

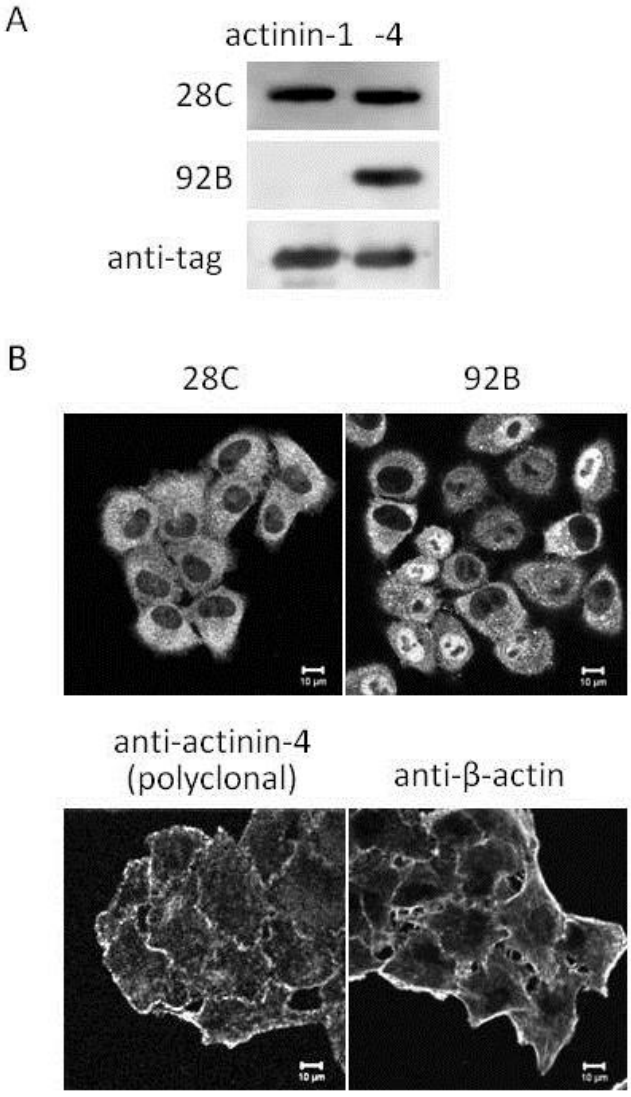

Fig. 6 Antibodies against actinins.
(A) Specificity for 28C and 92B against actinin-1 and actinin-4. His-tagged actinin-1 and actinin-4 were expressed in E. coli and applied for immunodetection. (B) Immunostaining results of HeLa cells by 28C, 92B, anti-actinin-4 polyclonal antibody, and anti-β-actin antibodies. Scale bars: 10 μm.

Discussion

The spectrum of the antigens recognized by our monoclonal antibodies largely overlapped with the components of nuclear matrix and mitotic chromosomal proteins identified by mass spectrometry (Table 1). These monoclonal antibodies obtained in this research will be useful to complement the proteomic research by providing molecular insights into the subcellular scaffolds. On the other hand, we did not obtain any antibodies against abundant proteins such as actin and tubulins, which are expected to be enriched in immunogens. Most of the identified antigens contain characteristic α-helix-based structural motifs such as coiled-coil and spectrin-repeat, which are the assemblies of double and triple α-helices (Table 1). We propose that such helix-based structures are highly antigenic. Anti-TCOF1 monoclonal antibody was generated previously from a mass production of monoclonal antibodies against hNopp140-associated proteins [16], also suggesting that this protein has highly antigenic properties. Although the immunogens might contain contamination of cytoplasmic proteins and some antibodies might be raised against those contaminations, we found many useful antibodies to reveal novel molecular dynamics in the nucleus. In addition, such antibodies uncover filamentous or non-filamentous molecular states of the antigens because of their monoclonalities, which correlated to the cytoplasmic and nuclear localizations of the antigens. These findings reconfirm the utility of the monoclonal antibodies which recognize specific molecular states, even they exhibits apparently unexpected immunofluorescence localizations.

Molecular mechanisms for the nuclear transport of macromolecules through the nuclear pore complex (NPC) had been described as size-filtering diffusion and karyopherin-dependent active transport [17]. The classical nuclear localization signal (NLS) serves as a general signal sequence that is recognized by importin-α/β for transport into the nucleus [18]. However, most of the cytoskeletal proteins identified as antigens, such as actinin and keratins, are larger than the diffusion limit and do not contain apparent NLS

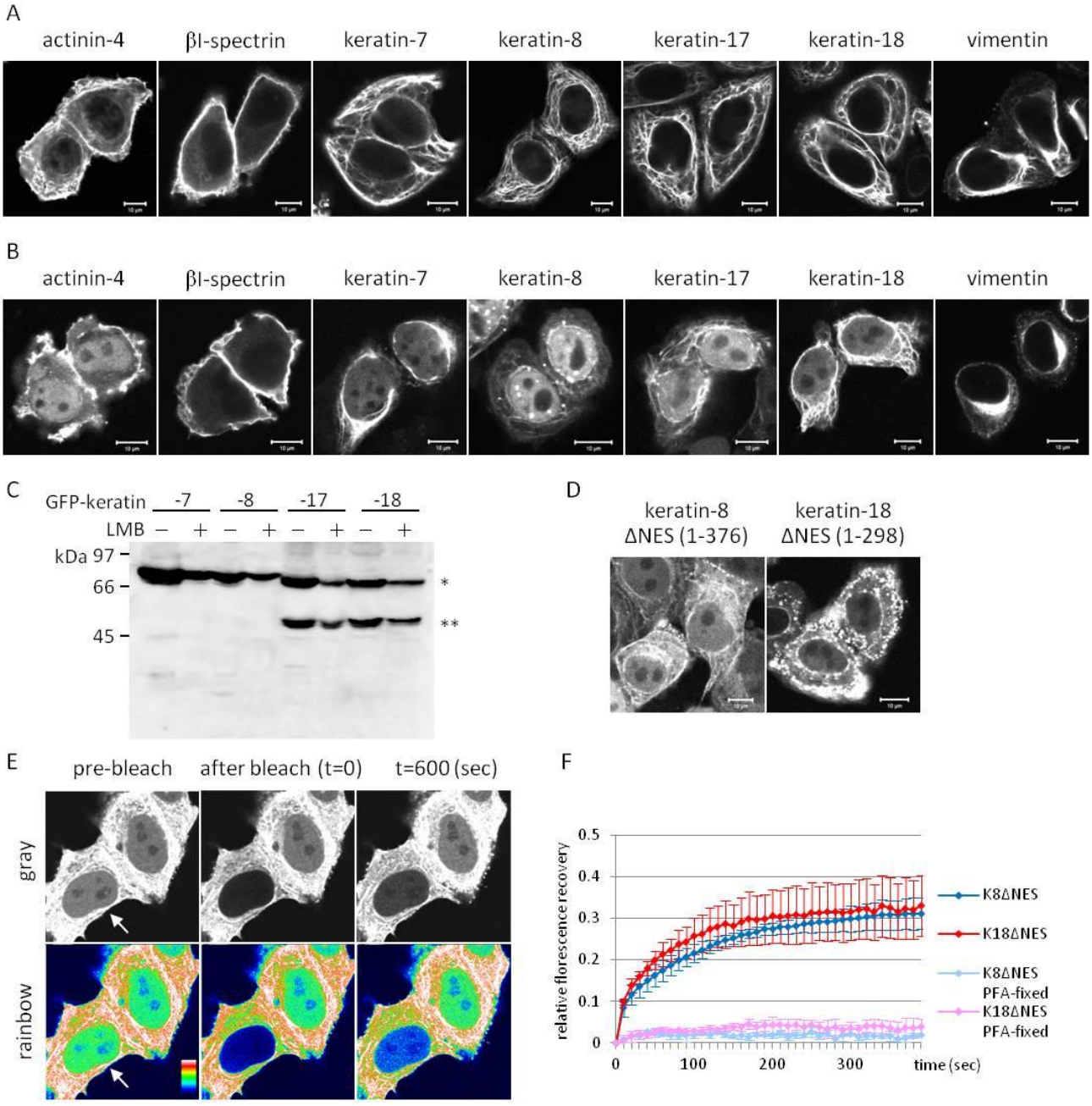

Fig. 7 CRM1-dependent nuclear localization of cytoskeletal components.
(A) GFP-fused cytoskeletal components were expressed in HeLa cells and the localization of fluorescent signals were observed 36 hours after transfection. Scale bars: 10 μm. (B) Subcellular localization of GFP-fused cytoskeletal components in HeLa cells treated with 20 ng/ml Leptomycin B for 24 hours before observation. (C) Western blot analysis of HeLa cell lysate expressing GFP-fused proteins with an anti-GFP antibody. *: full-length, **: degradation product. (D) Subcellular localization of GFP-fused keratin-8 and -18 lacking NES-containing portions. Scale bars: 10 μm. (E) Snapshots of FRAP analysis. Nuclear population of GFP-keratin-8 ΔNES (1-376) was bleached and the fluorescent recovery was recorded. The targeted cell was indicated by an arrow. The images represents pre-bleach (left), immediately after bleach (middle) and 600 seconds after bleach (right). Images are shown in gray (upper panels) and rainbow (lower panels) scales. (F) Quantitative analysis of fluorescent recoveries of GFP-keratin-8 ΔNES (K8 Δ NES) and GFP-keratin-18 ΔNES (K18ΔNES). Measurements of the cells fixed with 4% paraformaldehyde (PFA) serve as negative controls. n=3, ±SD.

consensus sequences. The nuclear localization of these helix-based cytoskeletal proteins is due partly to their amphiphilic properties that enable spontaneous nucleocytoplasmic shuttling. Hydrophobic interactions of amphiphilic α-helices are one of the driving forces for configuring the coiled-coil and spectrin-repeat structures [19, 20]. The NPC forms a hydrophobic barrier inside the pore with its hydrophobic subunits to prevent free diffusion of large macromolecules through the pore [21]. In addition to the passive diffusion and karyopherin-dependent transport, several amphiphilic molecules spontaneously pass through the NPC in a karyopherin-independent manner [22], possibly by exposing hydrophobic amino acid residues on the outer surface of the molecule to adapt to the hydrophobic environment inside the NPC. It is assumed that this selective permeability of the NPC enables dynamic molecular exchange of helix-based scaffold proteins between cytoplasm and nucleoplasm.

In this study we demonstrated CRM1-dependent nuclear shuttling of several cytoskeletal proteins, though some proteins were shown to be insensitive to LMB treatment (Fig. 7). Some cytoskeletal proteins were known to shuttle into the nucleus with another transport mediator. One protein is actin, one of the main cytoskeletal components, which is also known to shuttle into the nucleus to play a variety of roles in the nucleus. Although actin contains NES consensus sequences, its nuclear level is mainly regulated in an

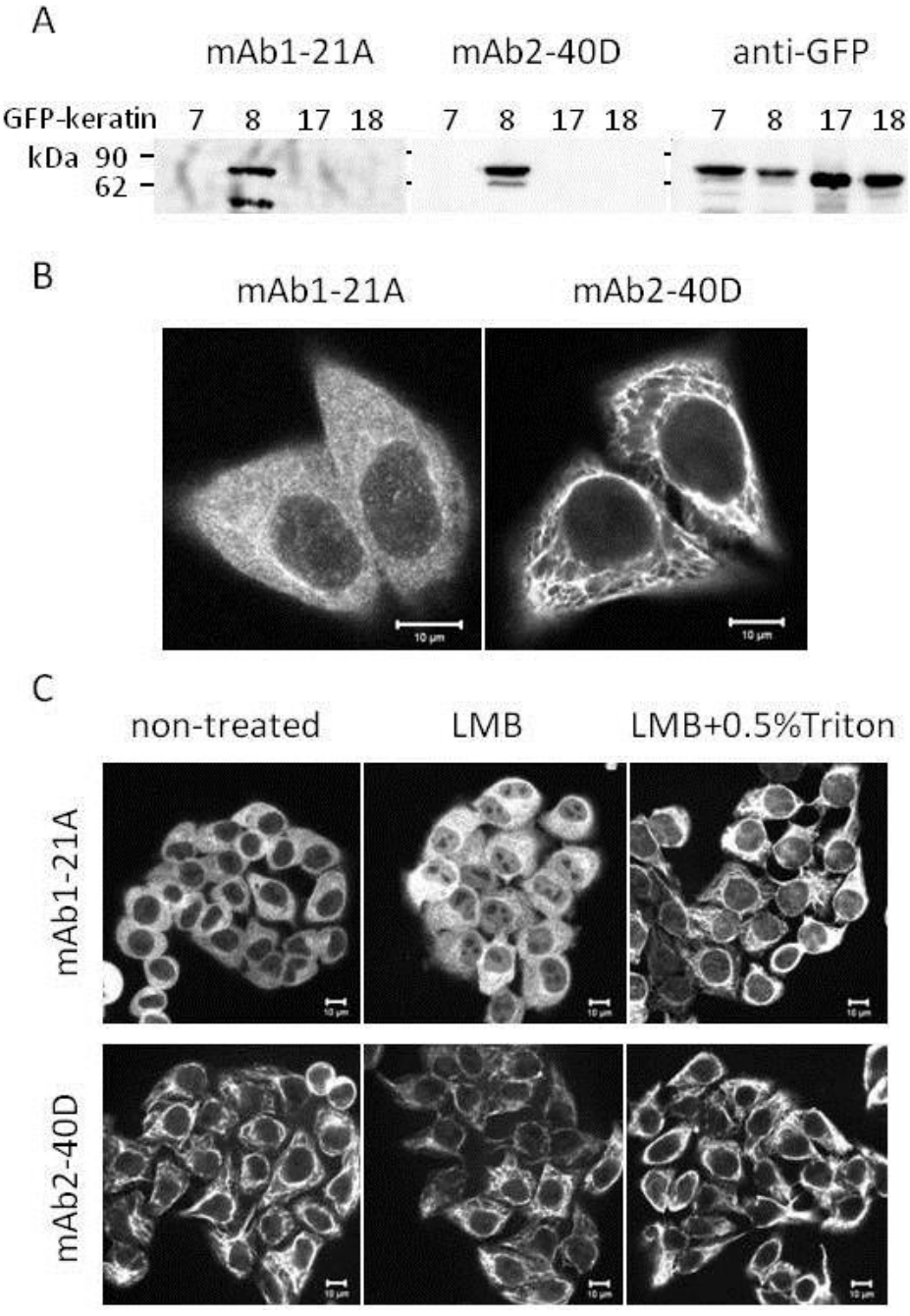

Fig. 8 Nuclear localization of non-filamentous keratin-8. (A) Western blot analysis of monoclonal antibodies 1-21A, 2-40D, and anti-GFP antibody against E. coli lysate expressing GFP-keratin-7, -8, -17, and -18. (B) Immuno-fluorescence staining of HeLa cells with 1-21A and 2-40D antibodies. (C) Immuno-staining of non-treated, LMB-treated (20 ng/ml, 2 hours), and LMB- and buffer A-treated HeLa cells with 1-21A and 2-40D antibodies. Scale bars: 10 μm.

exportin-6-dependent manner [23]. A variety of nuclear transport mediators would dynamically contribute to the spatiotemporal localization of scaffold proteins, reflecting the changing cellular requirements.

Besides its role as a physical scaffold for cells, cytoskeleton functions as a platform for many molecular interactions in the cytoplasm. The nuclear-localizing cytoskeletal components may also serve as a hub for the nuclear protein interactions. Interestingly, the nuclear populations of the shuttling proteins do not exhibit the same biochemical properties as their cytoskeletal states. For example, the nuclear keratin-8 was eluted by the detergent treatment (Fig. 8), demonstrating the highly soluble state of its nuclear population. Although the precise mechanisms regulating cytoskeletal protein molecular status in the nucleus remain unknown, their high solubility may be related to their role in the nucleus, such as, for example, the regulation of enzymatic reactions.

Contrary to actin filaments and microtubules, molecular events related to intermediate filaments have been described in less detail, possibly due to their highly insoluble properties, which prevent the use of typical molecular and biochemical approaches. Our antibody-based approach revealed the two distinctive populations of keratins as well as the nuclear localization of soluble keratins (Fig. 8). It has been reported that there are two distinctive populations of keratins, filamentous and free cytosolic pool, and that their dynamics, including the formation of the filament and their turn over, are regulated by specific phosphorylation [24, 25]. It is tempting to speculate what nuclear-specific keratin modification regulates its targeting and function in the nucleus. One example of a keratin whose role in the nucleus is known is keratin-17; it is involved in the Akt/mTOR signaling pathway by interacting with 14-3-3σ and it modulates the nucleocytoplasmic distribution of 14-3-3σ and regulates protein synthesis and cell growth [26]. Future studies will further examine the role of nuclear keratins in signal transduction, presumably by studying their interactions with nuclear factors.

As cytoskeletal organization serves as a sensor of extracellular environments, it is likely that dynamic nucleocytoplasmic shuttling of cytoskeletal components, including keratins, is important to orchestrate various cellular functions to achieve both basal and adaptive cellular responses.

Acknowledgements

During the last 12 years, many graduate students contributed to this work. We thank Dr. K. Fukui and Dr. S. Uchiyama for providing mitotic chromosomes, Dr. K. Ishii and Mr. Y. Hori for identifying antigens by HPLC and MASS techniques, Dr. K. Tsutsui for identifying anti-SAF-A antibodies, Dr. N. Takahashi for providing TCOF1 cDNA, Dr. Y. Taya for providing NuMA cDNA, and Mr. Y. Watanabe for the MASS analysis. This work was supported by Grants-in-Aid for Scientific Research on Innovative Areas “Spying minority in biological phenomena” (No.3306: 24115512) (to M.K.) from MEXT, Japan, and Scientific Research on Priority Areas “Nuclear Dynamics” (to K.T. and T.H.) from MEXT, Japan. M.K. and Y.H. were recipients of JSPS predoctoral fellowship.

References

1. Nickerson, J. A., Krockmalnic, G., Wan, K. M., and Penman, S. (1997). The nuclear matrix revealed by eluting chromatin from a cross-linked nucleus. *Proc Natl Acad Sci U S A* **94,** 4446-50.
2. Fey, E. G., Krochmalnic, G., and Penman, S. (1986). The nonchromatin substructures of the nucleus: the ribonucleoprotein (RNP)-containing and RNP-depleted matrices analyzed by sequential fractionation and resinless section electron microscopy. *J Cell Biol* **102,** 1654-65.
3. Yoshimura, S. H., Kim, J., and Takeyasu, K. (2003). On-substrate lysis treatment combined with scanning probe microscopy revealed chromosome structures in eukaryotes and prokaryotes. *J Electron Microsc (Tokyo)* **52,** 415-23.
4. Hirano, Y., Ishii, K., Kumeta, M., Furukawa, K., Takeyasu, K., and Horigome, T. (2009). Proteomic and targeted analytical identification of BXDC1 and EBNA1BP2 as dynamic scaffold proteins in the nucleolus. *Genes Cells* **14,** 155-66.
5. Ishii, K., Hirano, Y., Araki, N., Oda, T., Kumeta, M., Takeyasu, K., Furukawa, K., and Horigome, T. (2008). Nuclear matrix contains novel WD-repeat and disordered-region-rich proteins. *FEBS Lett* **582,** 3515-9.
6. Segawa, M., Niino, K., Mineki, R., Kaga, N., Murayama, K., Sugimoto, K., Watanabe, Y., Furukawa, K., and Horigome, T. (2005). Proteome analysis of a rat liver nuclear insoluble protein fraction and localization of a novel protein, ISP36, to compartments in the interchromatin space. *Febs J* **272,** 4327-38.
7. Kumeta, M., Yoshimura, S. H., Hejna, J., and Takeyasu, K. (2012). Nucleocytoplasmic

shuttling of cytoskeletal proteins: molecular mechanism and biological significance. *Int J Cell Biol* **2012,** 494902.
8. Miralles, F., and Visa, N. (2006). Actin in transcription and transcription regulation. *Curr Opin Cell Biol* **18,** 261-6.
9. Nelson, W. J., and Nusse, R. (2004). Convergence of Wnt, beta-catenin, and cadherin pathways. *Science* **303,** 1483-7.
10. Kumeta, M., Yoshimura, S. H., Harata, M., and Takeyasu, K. (2010). Molecular mechanisms underlying nucleocytoplasmic shuttling of actinin-4. *J Cell Sci* **123,** 1020-30.
11. Uchiyama, S., Kobayashi, S., Takata, H., Ishihara, T., Hori, N., Higashi, T., Hayashihara, K., Sone, T., Higo, D., Nirasawa, T., Takao, T., Matsunaga, S., and Fukui, K. (2005). Proteome analysis of human metaphase chromosomes. *J Biol Chem* **280,** 16994-7004.
12. Romig, H., Fackelmayer, F. O., Renz, A., Ramsperger, U., and Richter, A. (1992). Characterization of SAF-A, a novel nuclear DNA binding protein from HeLa cells with high affinity for nuclear matrix/scaffold attachment DNA elements. *Embo J* **11,** 3431-40.
13. Abad, P. C., Lewis, J., Mian, I. S., Knowles, D. W., Sturgis, J., Badve, S., Xie, J., and Lelievre, S. A. (2007). NuMA influences higher order chromatin organization in human mammary epithelium. *Mol Biol Cell* **18,** 348-61.
14. Wen, W., Meinkoth, J. L., Tsien, R. Y., and Taylor, S. S. (1995). Identification of a signal for rapid export of proteins from the nucleus. *Cell* **82,** 463-73.
15. Moll, R., Franke, W. W., Schiller, D. L., Geiger, B., and Krepler, R. (1982). The catalog of human cytokeratins: patterns of expression in normal epithelia, tumors and cultured cells. *Cell* **31,** 11-24.
16. Lin, C. I., and Yeh, N. H. (2009). Treacle recruits RNA polymerase I complex to the nucleolus that is independent of UBF. *Biochem Biophys Res Commun* **386,** 396-401.
17. Mohr, D., Frey, S., Fischer, T., Guttler, T., and Gorlich, D. (2009). Characterisation of the passive permeability barrier of nuclear pore complexes. *Embo J* **28,** 2541-53.
18. Mosammaparast, N., and Pemberton, L. F. (2004). Karyopherins: from nuclear-transport mediators to nuclear-function regulators. *Trends Cell Biol* **14,** 547-56.
19. O'Shea, E. K., Klemm, J. D., Kim, P. S., and Alber, T. (1991). X-ray structure of the GCN4 leucine zipper, a two-stranded, parallel coiled coil. *Science* **254,** 539-44.
20. Yan, Y., Winograd, E., Viel, A., Cronin, T., Harrison, S. C., and Branton, D. (1993). Crystal structure of the repetitive segments of spectrin. *Science* **262,** 2027-30.
21. Denning, D. P., Patel, S. S., Uversky, V., Fink, A. L., and Rexach, M. (2003). Disorder in the nuclear pore complex: the FG repeat regions of nucleoporins are natively unfolded. *Proc Natl Acad Sci U S A* **100,** 2450-5.
22. Kumeta, M., Yamaguchi, H., Yoshimura, S. H., and Takeyasu, K. (2012). Karyopherin-independent spontaneous transport of amphiphilic proteins through the nuclear pore. *J Cell Sci* **125,** 4979-84.
23. Stuven, T., Hartmann, E., and Gorlich, D. (2003). Exportin 6: a novel nuclear export receptor that is specific for profilin.actin complexes. *Embo J* **22,** 5928-40.
24. Omary, M. B., Ku, N. O., Liao, J., and Price, D. (1998). Keratin modifications and solubility properties in epithelial cells and in vitro. *Subcell Biochem* **31,** 105-40.
25. Ku, N. O., and Omary, M. B. (2000). Keratins turn over by ubiquitination in a phosphorylation-modulated fashion. *J Cell Biol* **149,** 547-52.
26. Kim, S., Wong, P., and Coulombe, P. A. (2006). A keratin cytoskeletal protein regulates protein synthesis and epithelial cell growth. *Nature* **441,** 362-5.